JOURNAL OF COMPUTATIONAL PHYSICS 9, 318–338 (1972)

Use of Numerically Inverted Laplace Transforms in Time-Dependent Transport Calculations*

JAMES H. RENKEN AND FRANK BIGGS

Sandia Laboratories, Albuquerque, New Mexico 87115

Received April 27, 1971

A time-dependent transport problem in which a monoenergetic point source emits a pulse of radiation into an infinite medium has been solved by Laplace transform techniques. Auxiliary information inferred from the physical nature of the problem is incorporated into the Laplace inversion procedure to eliminate the oscillatory solutions which usually result from attempts to numerically invert Laplace transforms. This simultaneous utilization of mathematical and physical information has made it possible to obtain credible time-dependent solutions for the transport problem under consideration.

1. INTRODUCTION

Solution of time-dependent transport problems by use of Laplace transform techniques is not a new idea [1]. The appeal of such an approach is quite obvious. Application of the Laplace transform to the time variable in the time-dependent transport equation produces an equation for the transform function which is formally identical with the time-independent transport equation. Hence, a reduction in dimensionality of the problem is achieved, and, in many instances, well-developed, time-independent methods may be used to solve for the transform of the particle flux.

There is one nearly insurmountable difficulty associated with the transform technique. In all but the most trivial problems, numerical methods must be used to solve for the transform function. This means that the transforms themselves are given as numerical values of finite accuracy at a limited number of values of the transform variable. Under these circumstances the unbounded nature of the Laplace inversion operator nearly always manifests itself, and conventional numerical-inversion schemes do not yield a credible time-dependent solution.

Considered as a strictly mathematical problem, numerical inversion of Laplace transforms is, for all practical purposes, an impossible task. Yet, in many physical

* Work performed under the auspices of the U. S. Atomic Energy Commission.

problems considerably more information than the transforms is known about the time-dependent solution. This information, which we designate as auxiliary information or constraints, includes knowledge of initial value and slope, asymptotic value, monotonicity, "smoothness," the integral of the function, etc. One of us (F.B.) has devised ways in which any available auxiliary information can be incorporated into the inversion procedure. The application of constraints usually serves to eliminate the unstable time-dependent solutions which are, to be sure, compatible with the imprecisely known transform values.

In Section 2, we consider the task of calculating transforms of the solution to a simple time-dependent transport problem. This problem consists of a point source with time-dependent intensity that is situated in an infinite medium. Several methods of solution have been used. The reasons for this redundancy are twofold. First, by comparing results from two different, but exact, methods the magnitude of the arithmetically introduced error in the transforms can be estimated. It is useful in the inversion procedure to have an idea of the absolute accuracy of the transforms. Second, the use of time-independent discrete-ordinates techniques on the same problem allows us to evaluate the feasibility of calculating usable transforms for a wide variety of time-dependent transport problems.

Section 3 presents the essential features of the numerical inversion methods. This method is a special application of a more general capability developed to solve numerically the Fredholm integral equation of the first kind. A more detailed and comprehensive description of this capability will be published elsewhere.

Finally, in Section 4 we present numerical results for the solution to the time-dependent problem we are considering. We compare our results with those obtained with cruder methods by other workers.

2. Calculation of the Laplace Transforms

As an example, we shall solve the following problem by the transform technique. Consider a point source which emits particles isotropically with a time-dependent strength of $S(t)$. The particles are assumed to be monoenergetic. The medium in which the source is located is homogeneous and infinite in extent, and it scatters particles isotropically without degrading their energies. For this problem the appropriate time-dependent transport equation is

$$[(1/v)(\partial/\partial t) + \boldsymbol{\Omega} \cdot \nabla + \sigma]\, \varphi(r, \boldsymbol{\Omega}, t) = \delta(r)\, S(t) + \frac{c\sigma}{4\pi} \int \varphi(r, \boldsymbol{\Omega}', t)\, d\boldsymbol{\Omega}', \quad (1)$$

with the condition that $\varphi = 0$ for $t \leqslant 0$. Recall that in one-dimensional spherical geometry

$$\boldsymbol{\Omega} \cdot \nabla = \mu(\partial/\partial r) + [(1 - \mu^2)/r](\partial/\partial \mu),$$

where μ is the dot product of Ω and the coordinate unit vector. Here, $\varphi(r, \Omega, t)$ is the flux of particles at r which are moving in direction Ω at time t, σ is the total interaction cross section, c is the ratio σ_s/σ, and σ_s is the scattering cross section.

Let us introduce the Laplace transform of φ defined by

$$\psi(r, \Omega, s) = \int_0^\infty \varphi(r, \Omega, t)\, e^{-st}\, dt. \tag{2}$$

Also, we define the Laplace transform of the source-strength time dependence to be

$$\mathscr{S}(s) = \int_0^\infty S(t)\, e^{-st}\, dt. \tag{3}$$

We now multiply Eq. (1) by e^{-st} and integrate over t from zero to infinity. We obtain as the equation for the transform

$$\left[\Omega \cdot \nabla + \left(\sigma + \frac{s}{v}\right)\right] \psi(r, \Omega, s) = \delta(r)\, \mathscr{S}(s) + \frac{c\sigma}{4\pi} \int \psi(r, \Omega', s)\, d\Omega'. \tag{4}$$

Notice that if we make the substitutions

$$\sigma + (s/v) \rightarrow \sigma',$$

$$\left[c \Big/ \left(1 + \frac{s}{v\sigma}\right)\right] \rightarrow c',$$

and

$$\mathscr{S}(s) \rightarrow S,$$

then the equation for the transform ψ,

$$[\Omega \cdot \nabla + \sigma']\, \psi(r, \Omega, s) = \delta(r)\, S + \frac{c'\sigma'}{4\pi} \int \psi(r, \Omega', s)\, d\Omega', \tag{5}$$

has exactly the same form as the time-independent transport equation for this problem. This development forms the basis for the statements in the introduction (Section 1).

Since the behavior of the unscattered flux is obtained trivially, we shall be concerned mainly with the time dependence of the scattered portion of the angle-integrated flux. The latter quantity is given by

$$\varphi_{\text{scat}}(r, t) = \varphi(r, t) - (e^{-\sigma r}/4\pi r^2)\, S[t - (r/v)], \tag{6}$$

where

$$\varphi(r, t) = \int_{4\pi} \varphi(r, \Omega, t)\, d\Omega. \tag{7}$$

The obvious relation of $\varphi(r, t)$ to the solution of Eq. (5) is

$$\psi(r, s) = \int_0^\infty \varphi(r, t)\, e^{-st}\, dt = \int_{4\pi} \psi(r, \mathbf{\Omega}, s)\, d\mathbf{\Omega}. \tag{8}$$

In the numerical work which is discussed next, we use $\sigma = 1$ cm^{-1}, $v = 1$ cm/sec, and $c = 0.3$. We further assume that the source is switched on instantaneously at $t = 0$ to an amplitude of 4 particles/sec and then abruptly switched off at $t = 0.25$ sec. For this behavior $\mathscr{S}(s)$ becomes

$$\mathscr{S}(s) = (4/s)[1 - e^{-s/4}]. \tag{9}$$

Case–deHoffmann–Placzek Solution

Case, deHoffmann, and Placzek (CdeHP) [2] present formulas and tables which allow the computation of numerical values for the solution of the steady-state point source problem with $S = \sigma = 1$. By appropriately scaling their results, numerical values for $\psi(r, s)$ can be obtained for a range of s values.

The scaling procedure is as follows. Aside from the spherical divergence, the transport solution depends upon the product σr. Therefore, to compute $\psi(R, s)$, we define an effective r and c such that

$$[\sigma + (s/v)]R = \sigma r_{\text{eff}} = r_{\text{eff}} \tag{10}$$

and

$$c_{\text{eff}} = c\Big/\Big(1 + \frac{s}{v\sigma}\Big) = c/(1 + s),$$

and use these effective values to find the transform from the results of CdeHP. The final step in determining $\psi(R, s)$ is to multiply the number obtained from CdeHP by $(r_{\text{eff}}/R)^2$ and $\mathscr{S}(s)$.

Although a few of the desired transform values could be derived directly from numbers tabulated by CdeHP, the majority had to be calculated from their formulas. Our computations were performed with a CDC-6600 computer. Except for their function $\epsilon(c, r)$ {Ref. [2, p. 76, Eq. (40)]}, wherever direct comparison was possible our numerical results agreed exactly with their tabulated values.

We numerically evaluated the integral which defines $\epsilon(c, r)$ in two ways. The first method was a standard adaptive Simpson's rule routine; the second method used a subdivided-interval, high-order Gaussian quadrature. These two methods produced function values which differed at most by one unit in the seventh significant figure. For certain values of the parameters, the CdeHP values for $\epsilon(c, r)$ listed in their Table 16 differed from our values by about 0.1 %.

The transform values of the scattered flux at radii of 3 and 6 cm as derived from the CdeHP results are listed in Table I.

TABLE I

Summary of the Scattered-Flux Transforms Calculated by Three Different Methods.

	$R = 3$ cm			$R = 6$ cm		
s	CdeHP	FS	DTF69	CdeHP	FS	DTF69
−0.70	2.52077(−2)[a]	—	2.45456(−2)	1.29144(−2)	—	1.21855(−2)
−0.60	8.12509(−3)	8.12509(−3)	8.12846(−3)	1.60331(−3)	1.60331(−3)	1.60275(−3)
−0.50	4.48782(−3)	4.48779(−3)	4.48584(−3)	5.54853(−4)	5.54853(−4)	5.53926(−4)
−0.40	2.69842(−3)	2.69841(−3)	2.69467(−3)	2.23433(−4)	2.23433(−4)	2.22741(−4)
−0.30	1.69301(−3)	1.69302(−3)	1.68892(−3)	9.67967(−5)	9.67968(−5)	9.63491(−5)
−0.25	1.35520(−3)	1.35521(−3)	1.35117(−3)	6.48407(−5)	6.48407(−5)	6.44881(−5)
−0.10	7.15484(−4)	7.15487(−3)	7.12076(−3)	2.04286(−5)	2.04287(−5)	2.02640(−5)
0	4.75742(−4)	4.75741(−4)	4.74765(−4)	9.72890(−6)	9.72889(−6)	9.67727(−6)
0.01	4.56997(−4)	4.56997(−4)	4.56034(−4)	9.04186(−6)	9.04188(−6)	8.99306(−6)
0.03	4.21823(−4)	4.21822(−4)	4.20887(−4)	7.81357(−6)	7.81357(−6)	7.76986(−6)
0.07	3.59795(−4)	3.59795(−4)	3.58917(−4)	5.84506(−6)	5.84506(−6)	5.81013(−6)
0.10	3.19635(−4)	3.19634(−4)	3.18800(−4)	4.70825(−6)	4.70825(−6)	4.67874(−6)
0.15	2.62840(−4)	2.62839(−4)	2.62079(−4)	3.29139(−6)	3.29139(−6)	3.26907(−6)
0.30	1.47697(−4)	1.47697(−4)	1.47139(−4)	1.14224(−6)	1.14224(−6)	1.13276(−6)
0.60	4.83335(−5)	4.83335(−5)	4.80573(−5)	1.44918(−7)	1.44917(−7)	1.43236(−7)
0.80	2.33962(−5)	2.33962(−5)	2.32294(−5)	3.75939(−8)	3.75939(−8)	3.70668(−8)
1.00	1.14541(−5)	1.14540(−5)	1.13551(−5)	9.90548(−9)	9.90548(−9)	9.74177(−9)
1.50	1.99197(−6)	1.99197(−6)	1.96626(−6)	3.70586(−10)	3.70586(−10)	3.61810(−10)
2.00	3.59385(−7)	3.59386(−7)	3.52946(−7)	1.45413(−11)	1.45413(−11)	1.40762(−11)
3.00	1.25441(−8)	1.25441(−8)	1.21598(−8)	2.44267(−14)	2.44267(−14)	2.31333(−14)
4.00	4.64882(−10)	4.64881(−10)	4.42907(−10)	4.40993(−17)	4.40994(−17)	4.05655(−17)
6.00	7.10928(−13)	7.10929(−13)	6.45157(−13)	1.62745(−22)	1.62745(−22)	1.37779(−22)
8.00	1.18999(−15)	1.18999(−15)	1.00556(−15)	6.64368(−28)	6.643 ·· (−28)	4.99537(−28)
10.00	2.11457(−18)	2.11456(−18)	1.86795(−18)	2.89404(−33)	2.8 ···· (−33)	2.31984(−33)
15.00	3.34098(−25)	3.34099(−25)	2.60118(−25)	1.37497(−46)	···	9.02760(−47)
20.00	6.19012(−32)	6.1899–(−32)	4.05910(−32)	7.71435(−60)	···	4.02450(−60)

[a] Interpret as 2.52077×10^{-2}.

Polynomial Expansion Solution

Another method by which transforms for our example can be calculated is the polynomial expansion method of Fano and Spencer (FS) [3–5]. Application of this method to the monoenergetic problem considered here is simpler than is treatment of the problems for which Fano and Spencer originally developed their method. We shall briefly outline the use of this method for our example.

It is advantageous to separate the total flux into unscattered and scattered components. Then the equation satisfied by the scattered flux transform is

$$[\Omega \cdot \nabla + \sigma'] \psi_s(r, \mu, s) = \frac{c'\sigma'}{2} \int_{-1}^{1} \psi_s(r, \mu', s)\, d\mu' + \frac{\mathscr{S}(s)\, \sigma' c'}{2} \frac{e^{-\sigma' r}}{4\pi r^2}. \quad (11)$$

To proceed, we express the scattered-flux transform as

$$\psi_s(r, \mu, s) = \sum_{l=0}^{\infty} \frac{2l+1}{2} N_l(r, s)\, P_l(\mu), \quad (12)$$

where $P_l(\mu)$ is a Legendre polynomial. Substitution of Eq. (12) into Eq. (11) and use of the orthogonality properties of the P_l enables us to derive

$$\frac{l+1}{2l+1}\left[\frac{l+2}{r} + \frac{\partial}{\partial r}\right] N_{l+1} - \frac{l}{2l+1}\left[\frac{l-1}{r} - \frac{\partial}{\partial r}\right] N_{l-1}$$
$$= c'\sigma' N_0 \delta_{l,0} - \sigma' N_l + c'\sigma' \mathscr{S}(s) \frac{e^{-\sigma' r}}{4\pi r^2} \delta_{l,0} \quad (13)$$

as the recursion relation for the N_l.

We define the moments of N_l to be

$$b_{l,n}(s) = \int_0^{\infty} r^n N_l(r, s)\, 4\pi r^2\, dr. \quad (14)$$

Using this definition in Eq. (13) we find that the moments are given by the interlinked hierarchy of equations

$$(2l+1)^{-1}\,[(l+1)(l-n)\, b_{l+1,n-1} - l(l+n+1)\, b_{l-1,n-1}]$$
$$= c'\sigma' b_{0,n} \delta_{l,0} - \sigma' b_{l,n} + c' \mathscr{S}(s)(\sigma')^{-n}\, n!\, \delta_{l,0}, \quad (15)$$

where in the derivation it is necessary to assume that no particles penetrate to $r = \infty$. Beginning with b_{00}, this expression can be solved for all the required moments.

We are interested in the integrated scattered-flux transform

$$\psi_s(r, s) = \int_{-1}^{1} \psi_s(r, \mu, s)\, d\mu = N_0(r, s). \tag{16}$$

To reconstruct $N_0(r, s)$ from the moments given by Eq. (15), we assume that the N_l can be written as

$$N_l(r, s) = \frac{y^l e^{-y}}{4\pi r^2} \sum_{n=0}^{\infty} a_{l,n}(s)\, W_n{}^l(y). \tag{17}$$

Here, $y = \sigma' r$ and the $W_n{}^l(y)$ are a set of biorthogonal polynomials which are discussed by Fano and Spencer [4]. By using the orthogonality properties of the $W_n{}^l(y)$ and their adjoints, we find that the coefficients $a_{l,n}(s)$ are related to the moments from Eq. (15) by

$$a_{l,n}(s) = \sum_{j=0}^{n} (\sigma')^{2j+l+1} \frac{(-1)^j}{(2j+2l)!} \binom{n}{j} b_{l,2j+l}(s). \tag{18}$$

Using the above formalism, we have calculated $N_0(r, s)$. Unfortunately, the sequence of partial sums generated by Eq. (17) does not converge rapidly. For most combinations of R and s, 30 to 50 terms in Eq. (17) sufficed to give six-figure convergence. Large values of s proved particularly difficult to treat. In these cases a 70-term series did not yield results with the desired accuracy. Since numerical problems, apparently due to finite accuracy of the CDC-6600 double-precision arithmetic, began to manifest themselves, we seem to have pursued this technique as far as possible. The transforms calculated by this method are also listed in Table I.

Discrete-Ordinates Solution

Although the previous two methods provide accurate transform values, it is of interest to calculate transforms by a method for which the restrictions on the nature of the physical problem are less severe. The method of discrete ordinates (MDO) [6] is a versatile and accurate numerical method for solution of a wide class of transport problems. For more general situations, it is just such a capability which is needed to solve the equivalent of Eq. (5).

We have calculated transforms for the problem considered here with the MDO as implemented by a computer program called DTF69 [7]. This code is a modification of the well-known DTF-IV program [8]. The results of the calculation are listed in Table I under the heading "DTF69."

Several comments about these transforms can be made. We observe that the $s = -0.7$ MDO values are relatively more inaccurate than the results for nearby

values of s. After performing calculations with several different radii for the necessarily finite spherical-transport region, we conclude that the cause of the discrepancy is due to the inadequate representation of an infinite medium by even a 33-mfp radius sphere. This effect is most pronounced for $s = -0.7$, since the cross-section augmentation essentially cancels the absorption, i.e., $c' = 1$, and we are left with a pure scattering problem. Because of machine storage limitations, it is difficult to use a radius large enough to mock up an infinite medium when no absorption is present.

In general, we see that there is reasonable agreement between the MDO values and those obtained by the other methods. After some computational experimentation we conclude that the observed divergence of transform values in Table I results from an increase in the effective total cross section as s increases. For very accurate results the MDO requires that the discrete-spatial intervals be a small fraction of a mean-free-path thick. As s increases the limitation of finite computer memory, even on a large machine, means this requirement can be satisfied less and less well. Although the number of spatial and angular intervals varied somewhat with s, at least 300 spatial intervals and 22 angular intervals were used in these calculations. This comparison indicates that calculation of very accurate transform values requires the use of as fine a discretization of space and angle as the computer capacity will allow.

Our MDO calculations treat the unscattered radiation analytically and use these results to compute first-collision sources in each spatial interval. In order to minimize any extraneous effects introduced when a finite-duration radiation pulse propagates through an artifically discretized spatial mesh, we have defined an averaging procedure to compute the Laplace transform of the source strength in each interval. Therefore, we feel it is unlikely that pulse propagation effects contribute much to the discrepancies displayed by the MDO numbers in Table I.

3. Numerical Inversion Procedure

Having obtained approximate values $\psi(r, s_i)$ for the Laplace transform at a finite number of points on the real s axis, we must now solve the integral equation

$$\psi(r, s) = \int_0^\infty \varphi(r, t)\, e^{-st}\, dt \tag{19}$$

for φ, the time-dependent scattered flux at r. This step is equivalent to obtaining the Laplace inversion of the transforms. Also at our disposal, we have some auxiliary information about the time dependence of φ and error information about the transforms. It is convenient to use retarded time as the independent

variable, i.e., $t = T - r/v$, where T is the real time. Since the time t is a real variable and $\varphi(t)$ is a real-valued function, we will be working entirely with real variables. We shall hereafter suppress, except as needed for clarity, any explicit dependence upon the distance r.

We have chosen a cubic spline to represent the early-time behavior of the flux since it is convenient to use and it adequately represents the expected features of the solution. It will be observed that the spline representation of the time-dependent solution yields transforms which differ from the original transforms only by amounts (residual error) which are comparable with the expected uncertainty in the original data.

Other representations of the early-time behavior are possible. However, to say that another representation is superior when it yields a residual error smaller than the uncertainty in the original data is not valid. Possibly the representation which requires the fewest parameters should be considered superior. We have not explored other alternatives.

For time-dependent transport in a finite-spherical medium, the solution is of the form [9]

$$\varphi(r, t) = \sum_{i=1}^{\infty} \alpha_i(r)\, e^{-\eta_i t}, \qquad \eta_i > 0. \tag{20}$$

This fact reinforces our intuitive feeling that in our problem a sum of exponentials would be a good representation of the late-time flux behavior. Thus we shall represent our final estimate of φ by a cubic spline function at early times and join to this at late times a two-term combination of exponentials.

Another piece of auxiliary information inferred from the physical nature of the problem is that φ increases monotonically and "smoothly" from zero at $t = 0$ to a maximum, and thereafter it decreases monotonically and "smoothly" to zero as $t \to \infty$. The term "smoothly" will be taken to mean that neither φ nor its first two time derivatives exhibit any oscillatory behavior.

We also observe that the final decay to zero goes as $\alpha_1(r)\, e^{-\eta_1 t}$, where η_1 is the smallest of the η_i. The error information is that the errors in the transform data are a few parts in 10^5 or better. Recall that $\psi(0)$ is the time-integrated flux.

In Fig. 1 we show a schematic of the flux $\varphi(t)$ on the left and its Laplace transform on the right. We note that some features in the time domain are identifiable in the transform domain. We call attention to the singularity at $s = -\eta_1$ in the transform domain.

Our approach is to use the auxiliary information to restrict the class of functions that are acceptable as estimates of φ. From the class of acceptable functions we select a "rough estimate." Then, through an iterative least-squares fitting procedure which involves constraints, smoothing, etc., we successively improve the estimate until the residual errors are consistent with the error information.

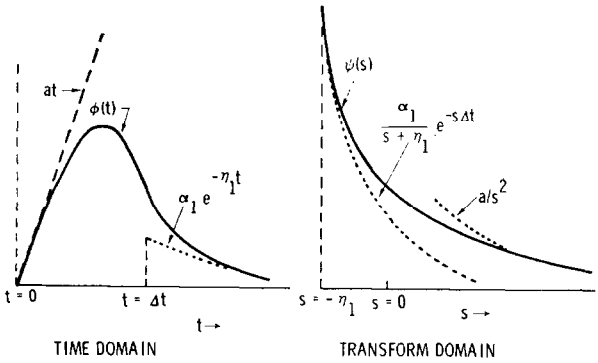

FIG. 1. Schematic of the flux $\varphi(t)$ and its Laplace transform $\psi(s)$.

In Phase I of the solution procedure, we select

$$\hat{\varphi}(t) = \begin{cases} at, & 0 \leqslant t \leqslant \nu \\ a\nu + b(t-\nu), & \nu \leqslant t \leqslant \beta \\ \alpha_1 e^{-\eta_1 t} + \alpha_2 e^{-\eta_2 t}, & \eta_1 < \eta_2\,, \quad \beta \leqslant t \end{cases} \tag{21}$$

as our "rough estimate" of $\varphi(t)$ and impose the condition that $\hat{\varphi}(t)$ be continuous in the interval $0 < t < \infty$. Note that $\hat{\varphi}(t)$ is a piecewise linear function for $t \leqslant \beta$ connected to a two-term exponential function for $t > \beta$.

The reason for selecting this form of "rough estimate" over a low-joint spline is that this function involves fewer parameters than, for example, a two-joint spline. We are assured this function will be in the class of acceptable functions, yet it is a sufficient estimate for this phase of the solution procedure.

The Laplace transform of $\hat{\varphi}$ is

$$\hat{\psi}(s) = \frac{(a-b)}{s^2}\gamma(2, \nu s) + \frac{b}{s^2}\gamma(2, \beta s) + \frac{\nu}{s}(a-b)(e^{-\nu s} - e^{-\beta s})$$

$$+ \frac{\alpha_1}{s+\eta_1} e^{-\beta(s+\eta_1)} + \frac{\alpha_2}{s+\eta_2} e^{-\beta(s+\eta_2)}, \tag{22}$$

where $\gamma(c, \chi)$ is the normalized incomplete gamma function [10].

The parameters a, ν, b, β, α_1, α_2, η_1, and η_2 are determined by minimizing the "residual error" term

$$Z_1 = \sum_{i=1}^{M} \left(\frac{\hat{\psi}_i - \psi_i}{\psi_i}\right)^2; \qquad \psi_i = \psi(s_i), \qquad \hat{\psi}_i = \hat{\psi}(s_i) \tag{23}$$

under the constraint that $\hat{\varphi}(t)$ be continuous in $0 < t < \infty$. This problem is

nonlinear in the parameters ν, β, η_1, and η_2. The BOTM [11] computer program

We now proceed to Phase II. Here we change the parametrization of the flux estimate to a function that consists of an N-joint cubic spline joined to a two-term exponential function at $t = \tau$ and require that the function and its first derivative be continuous at $t = \tau$. Analytically, this function is

$$\tilde{\varphi}(t) = \begin{cases} \sum_{k=1}^{4} C_k t^{k-1} + \sum_{k=5}^{N+4} C_k (t - J_{k-4})_+^3, & t \leqslant \tau \\ C_{N+5} e^{-\eta_1 t} + C_{N+6} e^{-\eta_2 t}, & t \geqslant \tau, \end{cases} \tag{24}$$

where J_m, $m = 1,\ldots, N$, are the abscissas of the cubic-spline joints (knots), $(x)_+^n = h(x)\, x^n$, where $h(x)$ is the Heaviside unit step function and η_1 and η_2 are the corresponding parameters obtained for the "rough estimate." The Laplace transform of $\tilde{\varphi}$ is

$$\tilde{\psi}(s) = \sum_{k=1}^{4} \frac{C_k}{s^k} \gamma(k, \tau s) + \sum_{k=5}^{N+4} C_k \frac{e^{-sJ_{k-4}}}{s^4} \gamma[4, s(\tau - J_{k-4})]$$

$$+ \frac{C_{N+5}}{s + \eta_1} e^{-\tau(s+\eta_1)} + \frac{C_{N+6}}{s + \eta_2} e^{-\tau(s+\eta_2)}, \tag{25}$$

where $\gamma(a, x)$ is again the normalized incomplete gamma function.

Now we define the quadratic form

$$Z_2 = \sum_{i=1}^{M} \left(\frac{\tilde{\psi}_i - \psi_i}{\psi_i} \right)^2 + \kappa \int_0^{\tau} W(t)(\tilde{\varphi}''(t))^2\, dt + \zeta \sum_{i=1}^{L} q_i(\tilde{\varphi}(t_i) - p_i)^2 \tag{26}$$

and designate the first term on the right side as the "residual-error" term, the second term as the "smoothing" term, and the last one as the "prior-estimate" term. With $\kappa = 0$ and $\zeta = 0$, the minimization of Z_2 would correspond to the method used in Phase I. The problem of solving for the $N + 6$ parameters C_k is a linear one, but with the number of parameters needed here it is usually not well conditioned enough so that an acceptable $\tilde{\varphi}$ is obtained. In order to generate some estimates $\tilde{\varphi}$ that are consistent with the auxiliary information, we use the "rough estimate" $\hat{\varphi}$ as a guide in selecting spline joints J_n, spline-exponential transition τ, and smoothing weight function $W(t)$. We set $\zeta = 0$ and minimize Z_2 for several values of κ while simultaneously imposing any equality constraints from the auxiliary information. At small κ, the resulting residual error is small, but the

oscillatory behavior of the resulting $\tilde{\varphi}$ is unacceptable. At large κ, a smooth $\tilde{\varphi}$ is obtained, but the residual error is large. It is usually necessary to repeat this procedure several times in order to establish the number of spline joints and their locations, the parameter τ, the smoothing weight $W(t)$, and to determine the range of values from which to select the optimum κ. Of all the candidates for $\tilde{\varphi}$ generated in this way, we select the ones that are consistent with all the auxiliary information, and among these we designate the one with the smallest residual error as the Phase II "good estimate." In Phase III of the solution procedure we use the parameters of the "good estimate" to calculate and then subtract from ψ the contribution to the Laplace transform coming from the spline part of the estimate $\tilde{\varphi}$. Then a function that is zero in $0 \leqslant t < \tau$ and a two-term exponential for $t \geqslant \tau$ is used to obtain transforms that are fitted to the above differences. The object here is to improve upon the accuracy of the parameters η_1 and η_2, but in this phase only four parameters must be determined.

In Phase IV we use the refined η_1 and η_2 from Phase III and again minimize Z_2 of Eq. (26). We use the smoothing weight function $W(t)$ together with the set of p_i corresponding to the "good estimate." We set κ equal to a smaller value than is used to obtain the "good estimate," select a set of weights q_i, and minimize Z_2 for a range of values of the parameter ζ. Again, we impose any equality constraints on this minimization that are provided by the auxiliary information. At small ζ the candidates are much the same as in Phase II. At large ζ the Phase II "good estimate" is obtained. Intermediate values of ζ provide a bountiful supply of good candidates for $\tilde{\varphi}$. This procedure stabilizes the least-squares problem when we increase the number of spline joints and increase the spline-exponential parameter τ. Of all the candidates for $\tilde{\varphi}$ generated in this way that are consistent with the auxiliary information, the one with the smallest residual error is selected as the Phase IV "better estimate."

Finally, an iteration is performed between Phases III and IV to improve the accuracy of the parameters η_1 and η_2 and to decrease the residual errors until they become consistent with the error information on the transform data. In Phase V, the p_k are changed from one iteration to the next to correspond to the best previous "better estimate." The q_k, the smoothing weight function $W(t)$, the parameter κ, the number and location of the spline joints, the parameter τ, etc., are varied as the situation dictates. The best of these "better estimates is designated as the "best estimate" and is taken as our final estimate $\tilde{\varphi}$ of the time-dependent flux φ.

4. Numerical Results

In this section we give numerical results for the time-dependent scattered flux at radii of 3 and 6 cm. Because of our desire to use the retarded-time scale, the appropriate values of ψ_i to use in Eq. (19) are obtained by multiplying the values

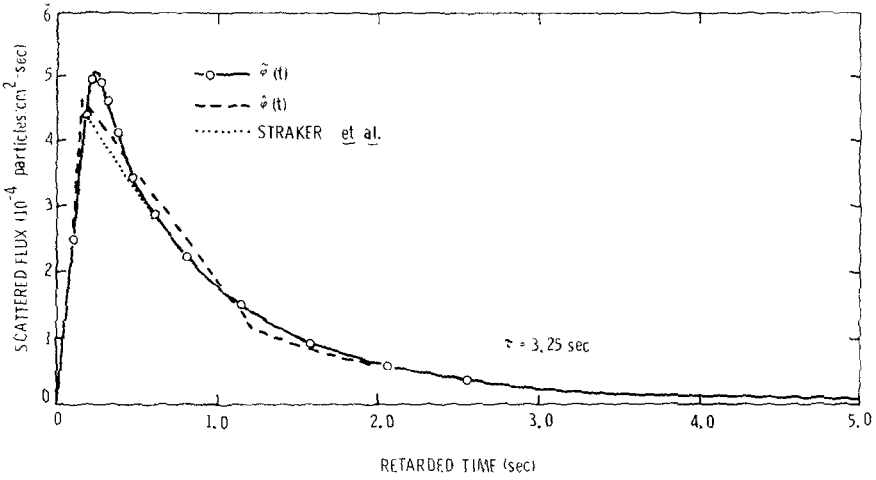

FIG. 2. Scattered flux vs time at $R = 3$ cm.

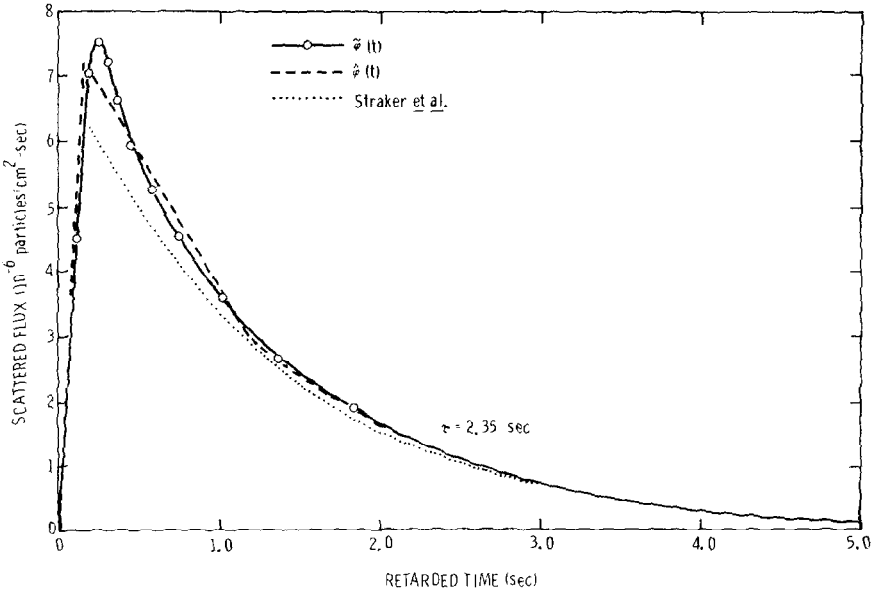

FIG. 3. Scattered flux vs time at $R = 6$ cm.

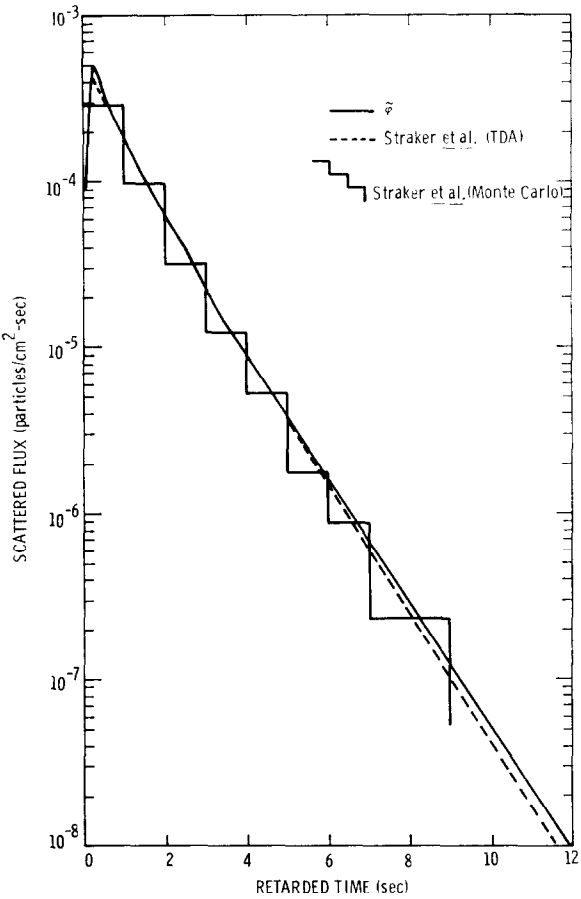

FIG. 4. Scattered flux vs time at $R = 3$ cm.

from the CdeHP column of Table I by the factor $\exp(rs_i/v)$. The Phase I estimate $\hat{\varphi}$ and the final estimate $\tilde{\varphi}$ are shown in Figs. 2 and 3 for the two radii in question. Also, for comparison, we show results for the same problem obtained by Straker et al. [12]. The circles on the graph of $\tilde{\varphi}$ show the spline-joint locations, and the spline-exponential transition time τ is written on the figures. The semilog plots of these data shown in Figs. 4 and 5 illustrate the late-time behavior of the solutions.

Table II lists the ψ_i and the relative residual errors $\Delta_i = (\tilde{\psi}_i/\psi_i - 1)$ vs s_i for radii of 3 and 6 cm, respectively. At the bottom of the residual-error columns the average and standard deviations of these errors are given.

The parameters for the "rough estimate" $\hat{\varphi}$ are given in Table III.

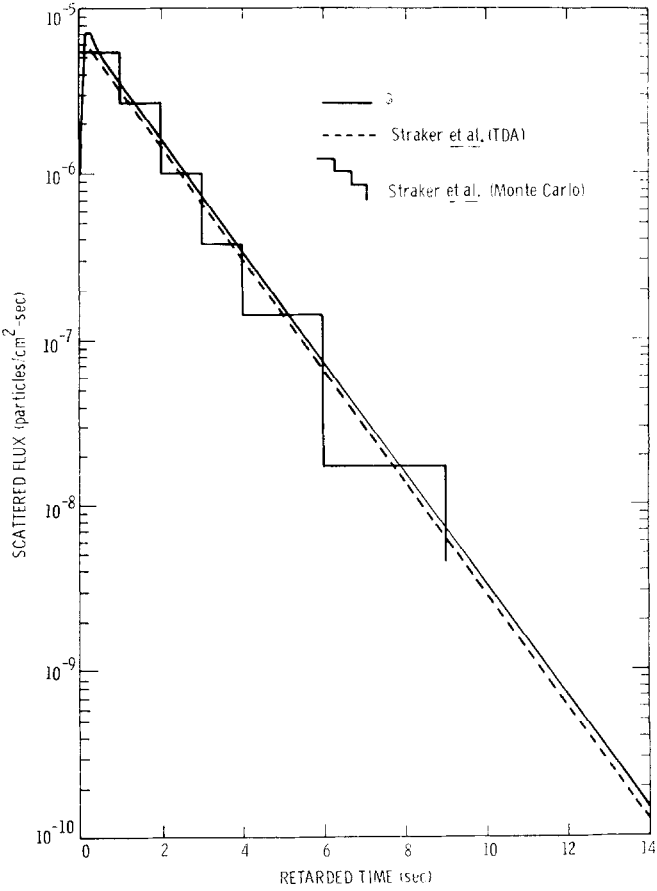

FIG. 5. Scattered flux vs. time at $R = 6$ cm.

The standard deviation of the relative residual errors $[\hat{\psi}(s_i)/\psi(s_i)] - 1$ is 2.97(−3) for $R = 3$ cm and 3.00(−3) for $R = 6$ cm. Note that there is more than a factor of one hundred decrease in the residual error in going from the "rough estimate" to the "best estimate."

The "best estimate" parameters are given in Table IV. The first four C' are used in the first sum of the first line of Eq. (24) and the next N C's and J's (joints) are for use in the second sum. The last two C's and the corresponding η's are for use in the exponential terms of Eq. (24). The parameter τ is the time where the spline function joins the exponential function. The parameters listed in Table IV may be used to evaluate $\tilde{\varphi}(t)$ for any time in $0 \leqslant t < \infty$. Their use in Eq. (25) provides the corresponding transforms $\tilde{\psi}(s)$.

TABLE II

Transforms $\psi(s)$ and the Relative Residual Errors $\Delta(s) = (\tilde{\psi}(s) - \psi(s))/\psi(s)$

	$R = 3$ cm		$R = 6$ cm	
S	$\psi(s)$	$\Delta(s)$	$\psi(s)$	$\Delta(s)$
−0.7	3.086845(−3)	1.80(−7)	1.936589(−4)	1.91(−7)
−0.6	1.343068(−3)	−2.83(−6)	4.380840(−5)	−3.18(−6)
−0.5	1.001368(−3)	−9.89(−6)	2.762450(−5)	−8.09(−6)
−0.4	8.127485(−4)	4.90(−5)	2.026938(−5)	3.98(−5)
−0.3	6.883265(−4)	−6.97(−6)	1.600039(−5)	−2.40(−6)
−0.25	6.401512(−4)	−2.83(−5)	1.446792(−5)	−1.79(−5)
−0.1	5.300436(−4)	−2.44(−5)	1.121145(−5)	−1.62(−5)
0	4.757420(−4)	−3.40(−6)	9.728900(−6)	−5.54(−6)
0.01	4.709146(−4)	1.31(−6)	9.600977(−6)	−7.97(−7)
0.03	4.615479(−4)	3.50(−6)	9.354542(−6)	1.22(−6)
0.07	4.438712(−4)	1.38(−5)	8.895957(−6)	6.99(−6)
0.1	4.314621(−4)	1.76(−5)	8.578991(−6)	1.09(−5)
0.15	4.122152(−4)	2.62(−5)	8.095513(−6)	1.71(−5)
0.3	3.632760(−4)	3.63(−5)	6.910149(−6)	3.04(−5)
0.6	2.924006(−4)	1.55(−5)	5.303743(−6)	1.48(−5)
0.8	2.579004(−4)	−7.77(−6)	4.568050(−6)	2.00(−6)
1.0	2.300617(−4)	−2.61(−5)	3.996156(−6)	−1.22(−5)
1.5	1.793114(−4)	−2.36(−5)	3.002889(−6)	−2.38(−5)
2.0	1.449863(−4)	4.23(−6)	2.366666(−6)	−6.50(−6)
3.0	1.016459(−4)	2.41(−5)	1.603856(−6)	1.85(−5)
4.0	7.566177(−5)	3.22(−6)	1.168152(−6)	1.15(−5)
6.0	4.667951(−5)	−1.58(−5)	7.016314(−7)	−1.52(−5)
8.0	3.152179(−5)	−2.90(−6)	4.661695(−7)	−6.91(−6)
10.0	2.259730(−5)	1.04(−5)	3.305015(−7)	1.20(−5)
15.0	1.167147(−5)	−3.25(−6)	1.678018(−7)	−2.81(−6)
20.0	7.069163(−6)	5.71(−7)	1.006091(−7)	3.61(−7)
	Mean = 1.95(−6) STD = 1.86(−5)		Mean = 1.71(−6) STD = 1.46(−5)	

TABLE III

Parameters for $\hat{\varphi}$ [see Eq. (21)]

Parameter	$R = 3$ cm	$R = 6$ cm
a	2.93(−3)	4.10(−5)
ν	0.16	0.18
b	−3.30(−4)	−4.08(−6)
β	1.23	1.18
α_1	1.02(−5)	9.81(−7)
α_2	3.3(−4)	6.81(−6)
η_1	0.708	0.708
η_2	0.898	0.796

TABLE IV

Fitting Parameters for Final Estimate $\tilde{\varphi}$

$R = 3$ cm		$R = 6$ cm	
	$C_1 = 0$		$C_1 = 0$
$N = 13$	$C_2 = 4.05068(-3)$	$N = 11$	$C_2 = 5.52262(-5)$
	$C_3 = -2.35676(-2)$		$C_3 = -2.88174(-4)$
	$C_4 = 9.52431(-2)$		$C_4 = 1.13575(-3)$
$J_1 = 0.1$	$C_5 = -1.53334(-1)$	$J_1 = 0.12$	$C_5 = -2.90423(-3)$
$J_2 = 0.18$	$C_6 = -2.66884(-2)$	$J_2 = 0.20$	$C_6 = 3.05189(-3)$
$J_3 = 0.22$	$C_7 = 1.71740(-1)$	$J_3 = 0.26$	$C_7 = -1.01685(-3)$
$J_4 = 0.275$	$C_8 = -7.56407(-2)$	$J_4 = 0.32$	$C_8 = -1.22888(-4)$
$J_5 = 0.32$	$C_9 = 2.94540(-2)$	$J_5 = 0.38$	$C_9 = -5.70141(-5)$
$J_6 = 0.375$	$C_{10} = -5.05784(-2)$	$J_6 = 0.46$	$C_{10} = -1.38091(-4)$
$J_7 = 0.47$	$C_{11} = 8.83922(-3)$	$J_7 = 0.58$	$C_{11} = 4.59749(-5)$
$J_8 = 0.61$	$C_{12} = 7.42776(-4)$	$J_8 = 0.76$	$C_{12} = 6.67894(-6)$
$J_9 = 0.81$	$C_{13} = 1.75028(-4)$	$J_9 = 1.02$	$C_{13} = -5.24669(-7)$
$J_{10} = 1.15$	$C_{14} = 2.85755(-5)$	$J_{10} = 1.37$	$C_{14} = -2.72443(-6)$
$J_{11} = 1.58$	$C_{15} = -4.06546(-5)$	$J_{11} = 1.84$	$C_{15} = 3.56594(-6)$
$J_{12} = 2.05$	$C_{16} = 6.89875(-5)$		
$J_{13} = 2.55$	$C_{17} = -6.44680(-6)$		
$\eta_1 = 0.716$	$C_{18} = 2.39516(-5)$	$\eta_1 = 0.710$	$C_{16} = 1.32408(-6)$
$\eta_2 = 0.898$	$C_{19} = 2.65638(-4)$	$\eta_2 = 0.806$	$C_{17} = 6.55704(-6)$
$\tau = 3.25$		$\tau = 2.35$	

5. Discussion

In the vicinity of the peak of the flux, our estimates $\tilde{\varphi}$ for both radii are significantly above those of Straker et al. (see Figs. 2 and 3). In Figs. 4 and 5 we show both the TDA (Time-Dependent ANISN) and Monte Carlo results of Straker et al. for the scattered flux. For $R = 3$ cm, our time-integrated scattered flux in the interval $0.2 \leqslant t \leqslant \infty$ is 2% below the Monte Carlo result and 1% above the TDA result. For the same quantities at $R = 6$ cm, our time-integrated scattered flux is 2% above the Monte Carlo result and 11% above the TDA result. We claim an accuracy of a few parts in 10^5 or better for our value of the time-integrated flux.

We verified the TDA code results of Straker et al. by repeating these calculations ourselves. Because of the way in which space must be discretized for these calculations, some error is introduced in the flux computed at the wavefront. On the basis of this and other experience with TDA, we feel that the differences between our results and those obtained with TDA are representative of the absolute accuracy of the TDA calculation.

We have used a cubic spline to parameterize in the interval $0 \leqslant t \leqslant \tau$ and contrained the function and its first two derivatives to be nonoscillatory. We did not constrain the third derivative to be nonoscillatory because the cubic-spline function has piece-wise constant third derivatives which are discontinuous at the spline joints. The actual flux φ has a continuous third derivative. Therefore, the third derivative of $\tilde{\varphi}$ would be expected, at best, to oscillate about the correct value. This effect is not noticeable in linear graphs such as Figs. 2 and 3; it is noticeable in the semilog plots of Figs. 4 and 5, especially at larger time where $\tilde{\varphi}$ is small and the spline joints are widely spaced. This effect can be diminished by using more joints or by going to a spline of higher degree.

We emphasize that the use of negative-s transforms has played a very important role in our treatment of this problem and was especially useful in establishing the exponents η_1 and η_2.

It is clear from Eq. (20) that the parameters η_1 and η_2 should be the same for all values of r. Our estimates of η_1 at $R = 3$ cm differ by less than 1 % from its estimate at $R = 6$ cm. We believe this difference in the η_1's is representative of the error in them. The η_2's differ because they are different weighted averages of all the larger η's which are not used in our approximation. This averaging effect may also have some effect on η_1.

In the Phase V iterations which yield the final order of magnitude of decrease in the residual errors, we increased the number of spline joints by a factor of two and increased the spline-exponential transition time τ by almost a factor of two. During these iterations the gross features of the estimate $\tilde{\varphi}$ changed relatively little (a few percent). This suggests that for most practical applications of this procedure, transform data to an accuracy of about 10^{-4} to 10^{-3} would be adequate, and an estimate $\tilde{\varphi}$ with about half as many joints could be used.

We can only guess at the accuracy of the estimate $\tilde{\varphi}$. From the last few Phase V iterations which involved changes in the joint locations, changes of less than 1 % in $\tilde{\varphi}$ were observed. This leads us to believe the spline portion of the estimate $\tilde{\varphi}$ is accurate to about a percent. We believe that the exponential decay parameter η_1 is accurate to within 1 %.

It is obvious that as the various iterations progressed this technique has involved much interaction between computer calculations and human judgment. Although we do not know how to eliminate this completely, we are working on some techniques that will enable the machine to take over more of the problem. The use of

some kind of graphical display with immediate turnaround would be extremely useful.

We turn now to a brief discussion of the nature of the intrinsic difficulty of this problem. Note that if the flux φ in the integrand of Eq. (19) is replaced by $(\varphi + A \cos \omega t)$, the left side of the equation becomes $\psi + As/(s^2 + \omega^2)$ which approaches ψ as $\omega \to \infty$. Our intuition senses this effect as the failure of the "smooth" kernel e^{-st} to resolve high frequencies. Another way to express the difficulty is to look at a real form of the inverse Laplace transform operator given by Widder [13]

$$\varphi(t) = \lim_{n\to\infty} \frac{(-1)^n}{n!} \left(\frac{n}{t}\right)^{n+1} \psi^{(n)}\left(\frac{n}{t}\right). \tag{27}$$

This operator is "unbounded" when applied to numerical values of ψ because it involves derivatives. In any attempt to invert the Laplace transform by using real-axis numerical data, the "unbounded" nature of the inversion operator manifests itself by giving rise to an ill-conditioned system to be solved numerically. The size of this system increases directly with the number of fitting parameters used in the flux estimate, and the ill conditioning increases drastically as the size of the system increases. We contend that in any approach to this problem that involves a least-squares minimization of residual errors, some kind of stabilizing influence must be used to cope with the ill-conditioned nature of the problem. We have provided this stabilizing influence by the use of constraints and the use of the "smoothing" and "prior-estimate" terms in Eq. (26) coupled with some auxiliary information about the flux φ and some error information on the transforms ψ.

Next we consider some statistics of the residual relative errors $\Delta_i = (\tilde{\psi}_i - \psi_i)/\psi_i$ of Table II. First, we simply assume that these errors correspond to independent samples drawn from a population where median is equal to zero. The chi-square test gives a probability of 0.70 for $R = 3$ and 1.0 for $R = 6$ that the resulting values of χ^2 be equaled or exceeded. We now assume that the Δ's correspond to independent samples drawn from a normal population with mean equal to zero. An estimate of the standard deviation is [14]

$$\text{STD} = \left(\frac{1}{n}\sum_{i=1}^{n} \Delta_i^2\right)^{1/2}, \qquad n = 26. \tag{28}$$

If we use this and the t-distribution with $n - 1$ degrees of freedom, we find probabilities of 0.60 and 0.56 for $R = 3$ and $R = 6$, respectively, and that the mean could deviate from zero as much as the observed values.

We now ask: What is the value of the population variance σ^2 that would give $\chi^2 = (1/\sigma^2) \sum \Delta_i^2$ which has a 0.05 probability of being exceeded ? Using 26 degrees

of freedom in the chi-squared distribution, we get $\sigma^2 = 2.31(-10)$ [$\sigma = 1.5(-5)$] and $\sigma^2 = 1.43(-10)$ [$\sigma = 1.2(-5)$] for $R = 3$ and $R = 6$, respectively, which is consistent with our error information on the transforms data.

We can also apply other tests. For example, if we divide the errors into "bins" and apply the chi-squared test, we find the observed residual errors Δ_i to be consistent with the assumption that they are drawn from a normal distribution centered at the origin with standard deviation as calculated by Eq. (28).

Finally, we have presented a set of transform data with an accuracy of a few parts in 10^5 or better, and we believe that the problem of unfolding estimates of the time-dependent flux from these data will provide a challenge to any unfold code.

ACKNOWLEDGMENTS

We wish to thank Ruth Lighthill and Joann Flinchum for computer-programming assistance. Thanks are due to D. E. Amos of Sandia Laboratories for supplying useful computer subroutines and for reading and commenting on this paper. David K. Kahaner and Bill Roach of the Los Alamos Scientific Laboratory kindly read an early draft of this paper and made helpful comments.

REFERENCES

1. K. M. CASE, F. DE HOFFMANN, AND G. PLACZEK, "Introduction to the Theory of Neutron Diffusion," Vol. I, p. 47, U. S. Government Printing Office, Washington, D.C., 1953.
2. K. M. CASE, F. DE HOFFMANN, AND G. PLACZEK, "Introduction to the Theory of Neutron Diffusion," Vol. I, p. 76, U. S. Government Printing Office, Washington, D. C., 1953.
3. LEWIS V. SPENCER AND U. FANO, *J. Res. Natl. Bur. Std. (U.S.)* **46** (1951), 446–456.
4. U. FANO, L. V. SPENCER, AND M. J. BERGER, "Handbuck der Physik," Vol. XXXVIII/2, p. 734, Springer-Verlag, Berlin, 1959.
5. J. H. RENKEN, "Transmission of X Rays Through Air," Sandia Laboratories, Albuquerque, New Mexico, SC-RR-65-141, 1965.
6. B. G. CARLSON AND K. D. LATHROP, Transport theory—the method of discrete ordinates, *in* "Computing Methods in Reactor Physics," Chap. III, Gordon and Breach, New York, 1964.
7. J. H. RENKEN AND K. G. ADAMS, "An Improved Capability for Solution of Photon Transport Problems by the Method of Discrete Ordinates," Sandia Laboratories, Albuquerque, New Mexico, SC-RR-69-739, 1969.
8. K. D. LATHROP, "DTF-IV, A FORTRAN-IV Program for Solving the Multigroup Transport Equation with Anisotropic Scattering," Los Alamos Scientific Laboratory, Los Alamos, New Mexico, LA-3373, 1965.
9. G. M. WING, "An Introduction to Transport Theory," p. 152, John Wiley and Sons, New York/London, 1962.
10. M. ABRAMOWITZ AND I. A. SEGUN, "Handbook of Mathematical Functions," p. 260, Dover Publications, Inc., New York, 1968.

11. M. S. SHAPIRO AND M. GOLDSTEIN, "A Collection of Mathematical Computer Routines," Courant Institute of Mathematical Sciences, New York University, New York, NYO-1480-14, 1965.
12. E. A. STRAKER, W. W. ENGLE, JR., AND P. N. STEVENS, "Some Calculated Milestone Solutions to Time-Dependent Radiation Transport Problems," Oak Ridge National Laboratory
14. HAROLD CRAMER, "Mathematical Methods of Statistics," p. 484, 485, Princeton University Press, Princeton, N. J., 1946.